This article has been accepted for publication in a future issue of this journal, but has not been fully edited. Content may change prior to final publication. Citation information: DOI 10.1109/TSP.2016.2521609, IEEE Transactions on Signal Processing

Broadbeam for Massive MIMO Systems

Deli Qiao, Haifeng Qian, and Geoffrey Ye Li

Abstract

Massive MIMO has been identified as one of the promising disruptive air interface techniques to address the huge capacity requirement of 5G wireless communications. For practical deployment of such systems, the control message needs to be broadcast to all users reliably in the cell using broadbeam. A perfect broadbeam is expected to have the same radiated power in all directions to cover users in any place in a cell. In this paper, we will show that there is no non-trivial solution for perfect broadbeam. Therefore, we develop a method for generating broadbeam that can allow tiny fluctuation in radiated power. Overall, this can serve as an ingredient for practical deployment of the massive MIMO systems.

I. Introduction

The requirements and potential techniques of the 5th generation (5G) wireless networks have attracted the interest of both the academia and the industry recently. It is expected that 5G could address the massive capacity and massive connectivity challenges brought by the exponentially growing mobile traffic and machine type applications [1]. A massive MIMO system [2] is formed by equipping a large number of transmit antennas at the base station. It can serve a large number of users simultaneously. Therefore, massive MIMO has been identified as a promising technique to address the challenges in 5G networks [4].

In a massive MIMO system, the number of transmit antennas can be as large as hundreds or even thousands, which is a couple of orders larger than the current 4th generation networks (typically 4 to 8 antennas at most). The increase in the transmit antenna number can introduce many benefits, such as capacity, multiplexing, diversity, and energy efficiency. However, there are also many potential challenges

D. Qiao and Haifeng Qian are with the School of Information Science and Technology, East China Normal University, Shanghai, China, 200241 (e-mail: dlqiao@ce.ecnu.edu.cn, hfqian@cs.ecnu.edu.cn). Geoffrey Ye Li is with the School of Electrical and Computer Engineering, Georgia Institute of Technology, Atlanta, Georgia 30332 (email:liye@ece.gatech.edu).

This work has been supported in part by the National Natural Science Foundation of China (61571191, 61572192) and the Science and Technology Commission of Shanghai Municipality (13JC1403502).

This article has been accepted for publication in a future issue of this journal, but has not been fully edited. Content may change prior to final publication. Citation information: DOI 10.1109/TSP.2016.2521609, IEEE Transactions on Signal Processing

for enabling massive MIMO [3]-[6]. Precoding design is an important topic for realizing the benefits of massive MIMO sytems [7]-[10]. Well-designed precoding vectors can reduce the required antenna number or transmit power to achieve certain performance [7], and reduce the peak-to-average power ratio (PAPR) [9], [10].

Generally, existing work on precoding design focuses on the OFDM systems [2]. However, there are still many problems open for practical deployment of massive MIMO-OFDM systems. One critical issue is how to design a broadbeam or a reliable control channel [11], such as Physical Downlink Control Channel (PDCCH) and Physical Broadcast Channel (PBCH) [12]. Otherwise, a large number of antennas may result in narrow beams [23]. As a result, some users in the cell may receive weak desired signal and strong inter-cell interference for the control message. In practice, the control signaling must be delivered to all users in the cell reliably. So it is desired to have a broadbeam with little or no variation in radiated power in all directions. In the current cellular networks, this can be achieved via sending control signaling with one antenna, for instance Cell-specific Reference Signaling (CRS) [12]. However, in massive MIMO systems, due to the low-power units, sending signal using only one antenna is extremely power inefficient. Therefore, new methods are expected to form reliable control channels. Antenna virtualization has been used in [13] to generate broadbeam. But the radiated power of the generated wide beam varies significantly in different directions.

In this work, we consider the problem of broadbeam design for massive MIMO systems with a uniform linear array (ULA) and a uniform rectangular array (URA). Note that beam pattern design has been an interesting topic for MIMO radar [14]-[20]. Generally, one can design the correlation matrix of the transmitted signal to synthesize the beam pattern. For instance, in [15], the problem of beam pattern design for a MIMO radar with ULA has been modeled as unconstrained minimization of a fourth order trigonometric polynomial, where constant modulus waveforms with the desired pattern have been derived by the quasi-Newton iterative algorithm. In [16], maximizing the power around the locations of interest and minimizing the cross-correlation of the signals reflected by the targets of interest have been proposed and an efficient semi-definite quadratic programming algorithm has been developed. In [17], an algorithm to synthesize transmit beam pattern in both space and frequency domains has been proposed for a ULA MIMO radar by decomposing the original optimization problem into two subproblems. In [18], beam pattern with energy focused on certain sectors for the direction of arrival (DOA) estimation has been designed by solving the optimazation problem over beamspace matrix. In certain cases, one can also design the beamforming vector, i.e., rank-1 beamformer, to synthesize the beam pattern. For instance, the rank-1 counterpart of beam pattern design has been discussed in [16]. In [19], both multi-rank and

This article has been accepted for publication in a future issue of this journal, but has not been fully edited. Content may change prior to final publication. Citation information: DOI 10.1109/TSP.2016.2521609, IEEE Transactions on Signal Processing

rank-1 beamformers, such as windowed steering vector and MVDR, for the beam design of MIMO radar with planar arrays have been presented. It has been shown in [20] that there are at most $2^{M-1}-1$ beamforming vectors generating the same beam pattern for a MIMO radar with ULA, where M is the antenna number.

In this paper, we consider broadbeam design for control channels in massive MIMO systems, and obtain the beamforming vectors for sending control signalling, which is similar to the rank-1 beamformer design for MIMO radar. Taking advantage of the method in [20], we further explore the properties of the potential beamforming vectors generating a perfect broadbeam to obtain some interesting findings and derive a method for designing a beamforming vector that can allow little fluctuation in radiated power. Note that unlike the MIMO radar, where the synthesized beams are incorporated for DOA estimation, the proposed broadbeam in this paper is adopted for control signalling transmission in massive MIMO systems.

In this paper, we investigate broadbeam generation for cellular systems with massive MIMO. We assume the ULA and URA at the base station. While beamforming vectors can be generated in [20] with the same beam pattern to that of a given beamforming vector, we will generate beamforming vectors with a specific beam pattern without any priori beamforming vector and further explore their properties. We first show that the generation of a perfect broadbeam can only result in trivial solutions. Therefore, some fluctuation must be allowed in the generated beam pattern. Then, we develop a method to find a beamforming vector with negligible ripples and a small peak-to-average power ratio (PAPR) or dynamic range (DR). The contributions of this paper can be summarized as follows:

1) We extend the method in [20] to obtain the beamforming vector given a target beam pattern without any priori beamforming vector, and prove that there are only trivial solutions to a perfect broadbeam.
2) We propose a method to obtain beamforming vectors with low PAPR or DR with negligible fluctuation in the beam pattern.
3) Through numerical evaluation, we demonstrate the effectiveness of the proposed method.

The organization of this paper is as follows. Section II presents the proposed method for generating broadbeam. In Section III, numerical examples are provided to show the effectiveness of the developed method. Finally, Section IV concludes this paper.

II. Broadbeam Design

In this section, we consider the design of broad beam for massive MIMO with a ULA and a URA, respectively. Based on the method in [20], we first show that there are only trivial solutions to generate

This article has been accepted for publication in a future issue of this journal, but has not been fully edited. Content may change prior to final publication. Citation information: DOI 10.1109/TSP.2016.2521609, IEEE Transactions on Signal Processing

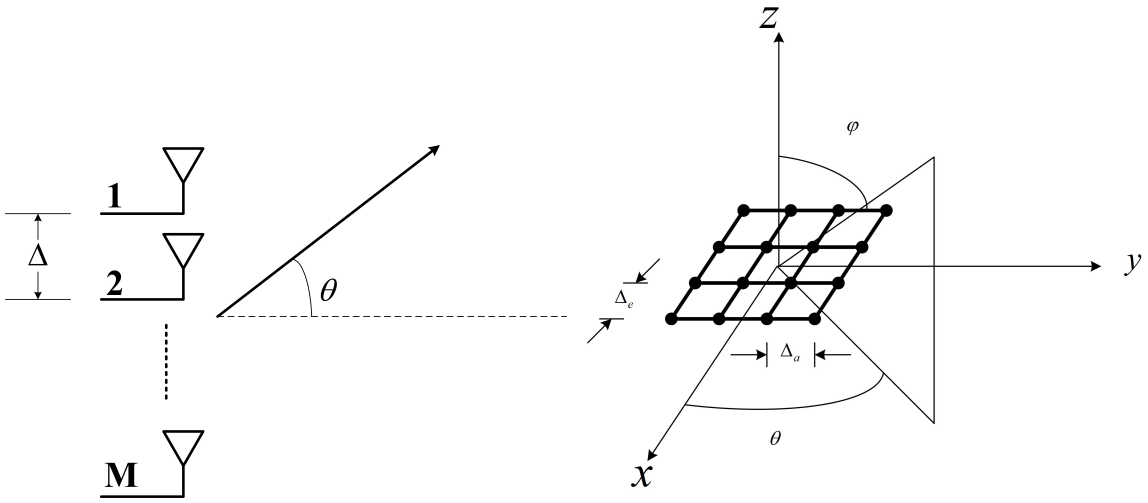

(a) ULA. (b) URA.

Fig. 1. Antenna structure.

a perfect broadbeam. Then, by allowing some fluctuation in the beam pattern, we propose a method to obtain beamforming vectors of low PAPR or DR, which can be applied in practical systems.

A. Uniform Linear Array

Consider a base station with M transmit antennas placed in a ULA as shown in Fig. 1(a), which is applicable in certain scenarios for massive MIMO systems [5]. The steering vector towards angle θ has the form [23]

$$\mathbf{a}(\theta) = [1 \quad a_2(\theta) \quad \cdots \quad a_M(\theta)]^T, \tag{1}$$

where $[\cdot]^T$ denotes the transpose of a matrix, and $a_m(\theta)$ represents phase shift of the signal at the mth antenna in relative to the first antenna with $a_1(\theta) = 1$. $a_m(\theta)$ depends on the antenna structure. For ULA,

$$a_m(\theta) = e^{j2\pi \frac{(m-1)\Delta}{\lambda} \sin(\theta)}, \tag{2}$$

where Δ is the antenna spacing and λ is the wavelength of the carrier.

Let $\mathbf{v} = [v_1, \ldots, v_M]^T \in \mathbb{C}^{M\times 1}$ denote the beamforming vector for generating the broadbeam. Then, the corresponding beam pattern generated is given by

$$f(\theta) = \mathbf{v}^H \mathbf{a}(\theta)\mathbf{a}^H(\theta)\mathbf{v}, \tag{3}$$

This article has been accepted for publication in a future issue of this journal, but has not been fully edited. Content may change prior to final publication. Citation information: DOI 10.1109/TSP.2016.2521609, IEEE Transactions on Signal Processing

where $[\cdot]^H$ denotes the Hermitian transpose of a matrix. The problem of designing a perfect broadbeam can be interpreted as

$$\begin{aligned} &\textbf{P1}: \\ &\quad \text{finding} \quad \mathbf{v} \\ &\quad \text{s.t. } f(\theta) = 1, \forall \theta \in [-\frac{\pi}{2}, \frac{\pi}{2}], \\ &\quad \text{and } \mathbf{v}^H\mathbf{v} = 1. \end{aligned} \tag{4}$$

It has been proven in [20] that there are at most $2^{M-1} - 1$ beamforming vectors generating the same beam pattern to a given beamforming vector. Taking advantage of the method in [20], we henceforth start from a target beam pattern in Problem **P1** instead, and further explore the properties of the beamforming vectors that can generate a perfect broadbeam. We have the following finding regarding the solutions to a perfect broadbeam.

Theorem. *For an arbitrary ULA antenna of size M, the only possible solutions for generating the perfect broadbeam are unit vectors, where only one element is with unit power while others are 0.*

Proof: Denote $\mathbf{D}(\theta) = \mathbf{a}(\theta)\mathbf{a}^H(\theta)$. Then,

$$f(\theta) = \mathbf{v}^H\mathbf{D}(\theta)\mathbf{v}. \tag{5}$$

Obviously, $\mathbf{D}(\theta)$ is a Toeplitz matrix. Denote the $2M-1$ elements generating the Toeplitz matrix $\mathbf{D}(\theta)$ as

$$\mathbf{w}(\theta) = \left[e^{-j2\pi(M-1)\frac{\Delta}{\lambda}\sin(\theta)}, e^{-j2\pi(M-2)\frac{\Delta}{\lambda}\sin(\theta)}, \ldots, 1, e^{j2\pi\frac{\Delta}{\lambda}\sin(\theta)}, \ldots, e^{j2\pi(M-1)\frac{\Delta}{\lambda}\sin(\theta)}\right]^T. \tag{6}$$

In that case, the matrix, $\mathbf{D}(\theta)$, can be expressed as $\mathbf{T}(\mathbf{w}(\theta))$, with $\mathbf{T}(\cdot)$ the generator for Toeplitz matrix.

Now, consider the beam pattern specified in Problem **P1** in (4). We can see that the radiated power is unit in all directions, that is, $f(\theta) = 1$ for all θ. To proceed, we need to choose a set of directions $\{\theta_1, \ldots, \theta_{2M-1}\}$ in $[-\frac{\pi}{2}, \frac{\pi}{2}]$. Then, we can obtain the following set of equations

$$\mathbf{v}^H\mathbf{T}(\mathbf{w}(\theta_k))\mathbf{v} = 1, \forall k = 1, 2, \ldots, 2M-1. \tag{7}$$

The linear combinations of the above set of equations with arbitrary choice of coefficients, $\mathbf{p}_i$ =

This article has been accepted for publication in a future issue of this journal, but has not been fully edited. Content may change prior to final publication. Citation information: DOI 10.1109/TSP.2016.2521609, IEEE Transactions on Signal Processing

$[p_{i1}, \ldots, p_{i,2M-1}]^T$, give us

$$\mathbf{v}^H \sum_{k=1}^{2M-1} p_{ik} \mathbf{T}(\mathbf{w}(\theta_k)) \mathbf{v} = \sum_{k=1}^{2M-1} p_{ik} = \Sigma_i, \tag{8}$$

where $\Sigma_i = \sum_{k=1}^{2M-1} p_{ik}$ is the sum of the elements of vector $\mathbf{p}_i$.

Since the Toeplitz matrix generator is a linear operation,

$$\sum_{k=1}^{2M-1} p_{ik} \mathbf{T}(\mathbf{w}(\theta_k)) = \mathbf{T}\left(\sum_{k=1}^{2M-1} p_{ik} \mathbf{w}(\theta_k) \right). \tag{9}$$

So, we can choose $\mathbf{p}_i$ such that all elements of the newly formed Toeplitz matrix are 0 except for the i-th diagonal elements. Note that, to make the diagonal elements of $\sum_{k=1}^{2M-1} p_{ik} \mathbf{T}(\mathbf{w}(\theta_k))$ become 0 except for the i-th diagonal, we only need to make sure that the element of $\sum_{k=1}^{2M-1} p_{ik} \mathbf{w}(\theta_k)$ are 0 except for the i-th one. Then, we can have the following set of equations

$$[\mathbf{w}(\theta_1)\, \mathbf{w}(\theta_2), \cdots, \mathbf{w}(\theta_{2M-1})]\, \mathbf{p}_i = \mathbf{e}_i,\ i = 1, \ldots, 2M-1. \tag{10}$$

where $\{\mathbf{e}_i\}$ is a unit vector with 1 for the i-th element and 0 else-where.

Let $\mathbf{P} = [\mathbf{p}_1, \ldots, \mathbf{p}_{2M-1}]$, and $\mathbf{W} = [\mathbf{w}(\theta_1), \cdots, \mathbf{w}(\theta_{2M-1})]$, we now have

$$\mathbf{WP} = \mathbf{I}, \tag{11}$$

where $\mathbf{I}$ is the identity matrix. With the choice of $\{\theta_k\}$ given above, $\mathbf{W}$ is a Vandermonde matrix. So, as long as $\{\theta_k\}$ does not lead to overlapping elements in $\{e^{-j2\pi \frac{\Delta}{\lambda} \sin(\theta_k)}\}$, $\mathbf{W}$ will be invertible. Note that this can be achieved by carefully choosing $\{\theta_k\}$. To facilitate the proof, we assume $\theta = 0$ as an sample. Without loss of generality, we choose $\{\theta_k\}$ such that $\sin(\theta_k) = \frac{2(k-M)}{2M-1}$, $k = 1, 2, \ldots, 2M-1$. Then, we have $\mathbf{P} = \mathbf{W}^{-1}$.

According to (8) and (10), we can have the following set of identities

$$v_1 v_M^* = \Sigma_1, \tag{12}$$

$$v_1 v_{M-1}^* + v_2 v_M^* = \Sigma_2, \tag{13}$$

$$\vdots$$

$$v_1 v_2^* + v_2 v_3^* + \cdots + v_{M-1} v_M^* = \Sigma_{M-1}, \tag{14}$$

$$|v_1|^2 + \cdots + |v_M|^2 = \Sigma_M \tag{15}$$

This article has been accepted for publication in a future issue of this journal, but has not been fully edited. Content may change prior to final publication. Citation information: DOI 10.1109/TSP.2016.2521609, IEEE Transactions on Signal Processing

where Σ_k is the sum of the elements of the k-th column of $\mathbf{W}^{-1}$. Denote the polynomial function

$$\Xi_i(x) = \sum_{k=1}^{2M-1} p_{ik} x^k. \tag{16}$$

By decomposing (11), we have

$$\Xi_i(e^{j2\pi \frac{\Delta}{\lambda}\left(\frac{2(k-M)}{2M-1}\right)}) = \begin{cases} 0, & \forall k \neq i, \\ 1, & k = i. \end{cases} \tag{17}$$

Obviously, we can get

$$\Sigma_i = \Xi_i(1) = \begin{cases} 0, & \forall i \neq M, \\ 1, & i = M. \end{cases} \tag{18}$$

Substituting the above results to equations (12)-(15), we can see that the only possible solutions are given by $|v_k| = 1$ for some k while $v_i = 0, \forall i \neq k$, proving the theorem. □

As shown in the above theorem, to achieve perfect broadbeam that radiates power identically in all directions, we can only let one antenna work. On the other hand, each antenna for massive MIMO systems is expected to be inexpensive, lower power components [5]. In this case, sending signal with only one antenna is extremely power inefficient, and fails to provide whole cell coverage.

If we allow the beam pattern to fluctuate in different directions within a very small amount, some useful broadbeams can be generated. Then, Problem **P1** can be modified into

$$\begin{aligned} &\mathbf{P2}: \\ &\quad \text{finding} \quad \mathbf{v} \\ &\quad \text{s.t.} \quad f(\theta) = 1 + \epsilon(\theta), \\ &\quad \text{and} \quad \mathbf{v}^H \mathbf{v} = 1. \end{aligned} \tag{19}$$

where $\epsilon(\theta)$ represents the fluctuation of the generated beam pattern with bounded support, i.e., $|\epsilon(\theta)| \leq \xi \ll 1$.

Remark 1. *ξ characterizes the fluctuation in broadbeam, which will lead to different levels of inter-cell interference. On the other hand, different choices of $\epsilon(\theta)$ generate different beam patterns while the spikes of the beam are constrained by ξ, and hence inter-cell interference. Intuitively, the smaller the number of the spikes the better performance. Therefore, we would like to choose $\epsilon(\theta)$ with at most one maximum value at $|\epsilon(\theta)| = \xi$. With this characterization of $\epsilon(\theta)$, there is little difference for any specific choice*

This article has been accepted for publication in a future issue of this journal, but has not been fully edited. Content may change prior to final publication. Citation information: DOI 10.1109/TSP.2016.2521609, IEEE Transactions on Signal Processing

of $\epsilon(\theta)$ as long as ξ and the number of spikes are constrained. In the following numerical results, we choose $\epsilon(\theta)$ as sinc-function of θ for instance.

Denote $r_k = 1 + \epsilon(\theta_k)$ for the set of $\{\theta_k\}$ chosen in the above proof. Then, (8) becomes

$$\mathbf{v}^H \sum_{k=1}^{2M-1} p_{ik} \mathbf{T}(\mathbf{w}(\theta_k))\mathbf{v} = \sum_{k=1}^{2M-1} r_k p_{ik} = \mathbf{r}^T \mathbf{p}_i \tag{20}$$

As a result, equations (12)-(15) can be expressed as

$$v_1 v_M^* = \mathbf{r}^T \mathbf{p}_1, \tag{21}$$

$$v_1 v_{M-1}^* + v_2 v_M^* = \mathbf{r}^T \mathbf{p}_2, \tag{22}$$

$$\vdots$$

$$v_1 v_2^* + v_2 v_3^* + \cdots + v_{M-1} v_M^* = \mathbf{r}^T \mathbf{p}_{M-1}, \tag{23}$$

$$|v_1|^2 + \cdots + |v_M|^2 = \mathbf{r}^T \mathbf{p}_{M.} \tag{24}$$

Similar to [20], the solutions to the above equation set can form

$$g(x) = \left(v_1 + v_2 x + \cdots + v_M x^{M-1}\right)\left(v_1^* + v_2^* x^{-1} + \cdots + v_M^* x^{-(M-1)}\right), \tag{25}$$

$$= \mathbf{r}^T \mathbf{p}_1 x^{-(M-1)} + \mathbf{r}^T \mathbf{p}_2 x^{-(M-2)} + \cdots + \mathbf{r}^T \mathbf{p}_M + \mathbf{r}^T \mathbf{p}_{M-1}^* x + \cdots + \mathbf{r}^T \mathbf{p}_1^* x^{M-1}. \tag{26}$$

From the structure of $g(x)$ in (25), if $x_1, x_2, \ldots, x_{M-1}$ are solutions to $g(x) = 0$, then $\frac{1}{x_1^*}, \frac{1}{x_2^*}, \ldots, \frac{1}{x_{M-1}^*}$ are too. From the solution set of $g(x) = 0$, we can form at most 2^{M-1} solutions of Problem **P2** by

$$\phi(x) = \prod_{m=1}^{M-1} (x - \alpha_m) = v_1 + v_2 x + \cdots + v_M x^{M-1}, \tag{27}$$

where $\alpha_m = x_m$ or $\frac{1}{x_m^*}$.

Even though Problem **P2** has at most 2^{M-1} solutions, we are interested in the one that achieves the lowest possible PAPR defined as

$$\delta = \frac{M \max_m |v_m|^2}{\| \mathbf{v} \|^2} \tag{28}$$

for the beamforming vector $\mathbf{v}$. Since there are 2^{M-1} possible beamforming vectors, exhaustive search can be used to find it.

Remark 2. *With the above characterization, we can see from (18) that $g(x) \equiv 1$ for perfect broadbeam*

This article has been accepted for publication in a future issue of this journal, but has not been fully edited. Content may change prior to final publication. Citation information: DOI 10.1109/TSP.2016.2521609, IEEE Transactions on Signal Processing

TABLE I
BROADBEAM GENERATION METHOD (BGM).

1. Choose $\epsilon(\theta)$;
2. Choose θ_k, $k = 1, \ldots, 2(M-1)$ such that $\sin(\theta_k) = \frac{2(k-M)}{2M-1}$;
3. Obtain the matrix $\mathbf{W} = [\mathbf{w}_1, \ldots, \mathbf{w}_{2M-1}]$, and the corresponding beam pattern vector $\mathbf{r} = [1+\epsilon(\theta_1), \ldots, 1+\epsilon(\theta_{2M-1})]^T$;
4. Solve the polynomials defined in (26) for solutions $\{x_1, \ldots, x_{M-1}, 1/x_1^*, \ldots, 1/x_{M-1}^*\}$;
5. Loop over all possible pairs of solutions to find the associated beamforming vector $\mathbf{v}$ specified in (27);
6. In the loop, save the beamforming vector $\mathbf{v}$ with lowest PAPR defined in (28);
7. The desired beamforming vector is given by $\frac{\mathbf{v}}{\|\mathbf{v}\|}$.

*generation, i.e., there is no solution to $g(x) = 0$. Therefore, we can not find 2^{M-1} solutions to Problem **P1** as we do for Problem **P2**.*

To summarize the above discussion, we propose the procedures in Table I to obtain the desired beamforming vector for generating a broadbeam.

Remark 3. *Note that given an antenna setting, the previous algorithm can be performed **off-line**. For very large M, 2^{M-1} can be extremely large. In this case, one can set certain target threshold for PAPR or DR, and stop the iteration when the threshold is achieved. In this way, the running time can be reduced.*

Here are some practical considerations in implementing the above method.

1) **Peak Power Constraint**: Moreover, in practical use, the antennas may be subject to a peak power constraint, i.e., $|v_m|^2 \leq v_{\max}$, $m = 1, 2, \ldots, M$. Then, we need to normalize the beamforming vector as follows

$$\frac{\mathbf{v}}{\max_m |v_m|}\sqrt{v_{\max}}. \tag{29}$$

In this case, the base station should radiate the power as much as possible. That is, we need to find a beamforming vector with maximum radiated power, i.e., $\| \mathbf{v} \|^2$. Note that this problem is equivalent to finding a beamforming vector with minimum PAPR defined in (28).

This article has been accepted for publication in a future issue of this journal, but has not been fully edited. Content may change prior to final publication. Citation information: DOI 10.1109/TSP.2016.2521609, IEEE Transactions on Signal Processing

2) **Dynamic Range**: Another metric of interest is the DR, which is defined as

$$\frac{\max_m |v_m|^2}{\min_m |v_m|^2}. \tag{30}$$

In this case, we would like to minimize the dynamic range. Compared with (28), we can see that the difference with PAPR-based method lies in the denominator, which is now the minimum power of the antennas.

B. Uniform Rectangular Array

Note that generating broadbeam for the URA is similar to the case of the ULA except that we need to consider the azimuth and elevation angles. Consider a uniform rectangular array with $M \times N$ identical antennas placed with uniform spacing as shown in Fig. 1(b). The component of the steering vector for each antenna in the direction (φ, θ) is given by [23]

$$[\mathbf{A}(\varphi,\theta)]_{mn} = a_{mn}(\varphi,\theta) = e^{j2\pi \frac{(m-1)\Delta_a}{\lambda} \sin(\varphi)\sin(\theta) + j2\pi \frac{(n-1)\Delta_e}{\lambda} \sin(\varphi)\cos(\theta)}. \tag{31}$$

Then, the steering vector can be written as

$$\mathbf{a}(\varphi,\theta) = \text{vec}(\mathbf{A}(\varphi,\theta)) = \mathbf{a}_a(\varphi,\theta) \otimes \mathbf{a}_e(\varphi,\theta), \tag{32}$$

where

$$\mathbf{a}_a(\varphi,\theta) = [1, e^{j2\pi \frac{\Delta_a}{\lambda} \sin(\varphi)\sin(\theta)}, \ldots, e^{j2\pi \frac{(M-1)\Delta_a}{\lambda} \sin(\varphi)\sin(\theta)}]^T,$$

and

$$\mathbf{a}_e(\varphi,\theta) = [1, e^{j2\pi \frac{\Delta_e}{\lambda} \sin(\varphi)\cos(\theta)}, \ldots, e^{j2\pi \frac{(N-1)\Delta_e}{\lambda} \sin(\varphi)\cos(\theta)}]^T.$$

This article has been accepted for publication in a future issue of this journal, but has not been fully edited. Content may change prior to final publication. Citation information: DOI 10.1109/TSP.2016.2521609, IEEE Transactions on Signal Processing

If we let $\mathbf{v} = \mathbf{v}_a \otimes \mathbf{v}_e$, the transmit beam pattern can be expressed as

$$
\begin{aligned}
f(\varphi,\theta) &= \mathbf{v}^H \mathbf{a}(\varphi,\theta)\mathbf{a}^H(\varphi,\theta)\mathbf{v} && (33)\\
&= (\mathbf{v}_a \otimes \mathbf{v}_e)^H (\mathbf{a}_a(\varphi,\theta) \otimes \mathbf{a}_e(\varphi,\theta)) \\
&\quad \cdot (\mathbf{a}_a(\varphi,\theta) \otimes \mathbf{a}_e(\varphi,\theta))^H (\mathbf{v}_a \otimes \mathbf{v}_e) && (34)\\
&= (\mathbf{v}_a^H \otimes \mathbf{v}_e^H)(\mathbf{a}_a(\varphi,\theta) \otimes \mathbf{a}_e(\varphi,\theta)) \\
&\quad \cdot (\mathbf{a}_a^H(\varphi,\theta) \otimes \mathbf{a}_e^H(\varphi,\theta))(\mathbf{v}_a \otimes \mathbf{v}_e) && (35)\\
&= (\mathbf{v}_a^H \mathbf{a}_a(\varphi,\theta)\mathbf{a}_a^H(\varphi,\theta)\mathbf{v}_a) \\
&\quad \otimes (\mathbf{v}_e^H \mathbf{a}_e(\varphi,\theta)\mathbf{a}_e^H(\varphi,\theta)\mathbf{v}_e) && (36)\\
&= (\mathbf{v}_a^H \mathbf{a}_a(\varphi,\theta)\mathbf{a}_a^H(\varphi,\theta)\mathbf{v}_a) \\
&\quad \cdot (\mathbf{v}_e^H \mathbf{a}_e(\varphi,\theta)\mathbf{a}_e^H(\varphi,\theta)\mathbf{v}_e) && (37)\\
&= f_a(\varphi,\theta) f_e(\varphi,\theta) && (38)
\end{aligned}
$$

where the following properties of Kronecker product are used: 1) $(A \otimes B)^H = A^H \otimes B^H$; 2) $(A \otimes B)(C \otimes D) = (AC) \otimes (BD)$, and (37) holds since both terms inside the parenthesis are scalar values, $f_a(\varphi,\theta) = \mathbf{v}_a^H \mathbf{a}_a(\varphi,\theta)\mathbf{a}_a^H(\varphi,\theta)\mathbf{v}_a$, and $f_e(\varphi,\theta) = \mathbf{v}_e^H \mathbf{a}_e(\varphi,\theta)\mathbf{a}_e^H(\varphi,\theta)\mathbf{v}_e$.

Then, similar to (4), we can interpret the problem of designing broadbeam for the URA as[1]

$$
\begin{aligned}
&\textbf{P3}: \\
&\quad \text{finding} \quad \mathbf{v} \\
&\qquad \text{s.t. } f(\varphi,\theta) = 1, \forall \varphi \in [-\frac{\pi}{2}, \frac{\pi}{2}], \theta \in [-\frac{\pi}{2}, \frac{\pi}{2}], \\
&\qquad\quad \text{and } \mathbf{v}^H \mathbf{v} = 1.
\end{aligned} \tag{39}
$$

Combining (38), we can decompose the previous problem into two subproblems of finding $\mathbf{v}_a$ and $\mathbf{v}_e$ with $f_a(\varphi,\theta) = 1$ and $f_e(\varphi,\theta) = 1$ as constraints, respectively. Note that they are similar to the discussion for the ULA, and hence the Theorem holds for the URA as well. Also we can design beamforming vectors that can allow some fluctuations in radiation pattern following similar steps.

[1]If downtilt is taken into account [21], the ideal beam pattern may not be the broadbeam with identical radiated power in different directions. However, finding the ideal pattern seems intractable, and is beyond the focus of this paper. We would like to note here that broadbeam is still a viable solution for the design of control channel.

This article has been accepted for publication in a future issue of this journal, but has not been fully edited. Content may change prior to final publication. Citation information: DOI 10.1109/TSP.2016.2521609, IEEE Transactions on Signal Processing

III. Numerical Results

In this section, we first evaluate the beam pattern of the proposed method for the ULA and the URA, respectively. We also investigate the impact of ξ on the resulting performance in terms of PAPR and DR for further findings. Moreover, we illustrate the effectiveness of the proposed broadbeam over massive MIMO systems considered in [2] through comparison with sending control signalling by random beamforming, one antenna under full and $1/M$ power constraints, respectively.

A. Beam Pattern

In this part, we will evaluate the proposed method for generating a broadbeam. We consider two different performance metrics, PAPR and DR. In the following figures, "PAPR-based" refers to the method with PAPR as the optimization metric while "DR-based" refers to the method with dynamic range as the optimization metric.

Consider a ULA with 16 antennas with $\Delta = \frac{1}{2}\lambda$. Assume $\xi = 0.01$. The PAPR obtained is $\delta = 2.37 = 3.75$ dB while the minimum dynamic range is 28 dB. In Fig. 2, we plot the corresponding power of each antenna. In the figure, the circles and squares represent the power of different antennas with the PAPR-based or DR-based optimization method, where the dashed line represent the perfect scenario with PAPR $\delta = 1 = 0$ dB, i.e., constant envelope with $\frac{1}{16}$. In Fig. 3, we plot the associated beam pattern for the PAPR-based method. Note that the beam pattern associated with the DR-based method is the same as that of the PAPR-based method considering (19), and hence is omitted here. As we can see from the figure, the beam pattern for the generated beamforming vector is almost flat for $-90^o \leq \theta \leq 90^o$.

We are also interested in the total radiated power with the broadbeam in the presence of additional peak power constraints on antennas. Here, we assume that the peak power is $v_{\max} = \frac{1}{M} = \frac{1}{16}$. We plot the total radiated power in percentage with respect to the full power of 1 as a function of ξ in Fig. 4. From the figure, the overall trend for radiated power is increasing with ξ, since smaller ξ generally requires the antennas to counteract the interactions between each other more stringently, which may waste more power. Note that if we send signal with only single antenna, the power radiated is $\frac{1}{16} = 6.25\%$. We can obtain a significant boost in radiated power with the proposed method, e.g., 9 dB increase at $\xi = 0.04$ where around 50% of the total power can be radiated, and hence in the coverage range. And it is not surprising that reducing dynamic range wastes more power. In addition, we plot the dynamic range as a function of ξ in Fig. 5. From the figure, the overall trend for dynamic range is decreasing with ξ.

This article has been accepted for publication in a future issue of this journal, but has not been fully edited. Content may change prior to final publication. Citation information: DOI 10.1109/TSP.2016.2521609, IEEE Transactions on Signal Processing

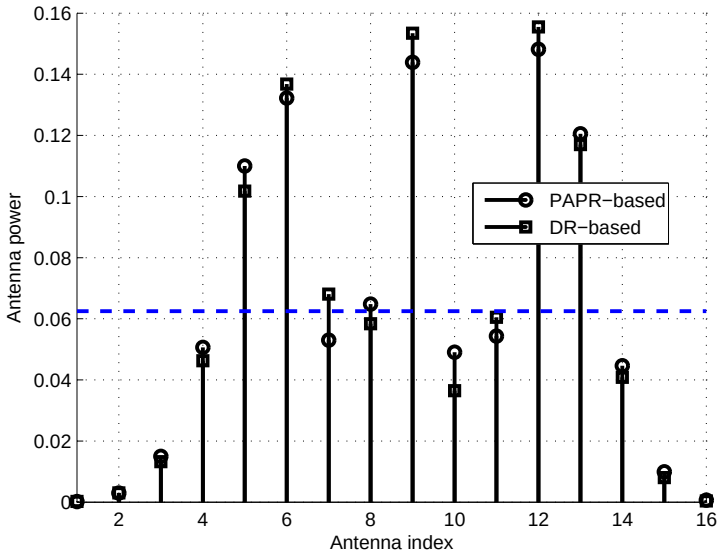

Fig. 2. Power of each antenna. $M = 16$. $\xi = 0.01$.

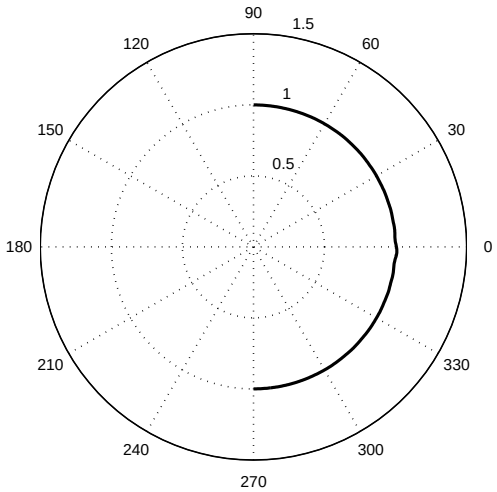

Fig. 3. Beam pattern. PAPR-based. $M = 16$.

This article has been accepted for publication in a future issue of this journal, but has not been fully edited. Content may change prior to final publication. Citation information: DOI 10.1109/TSP.2016.2521609, IEEE Transactions on Signal Processing

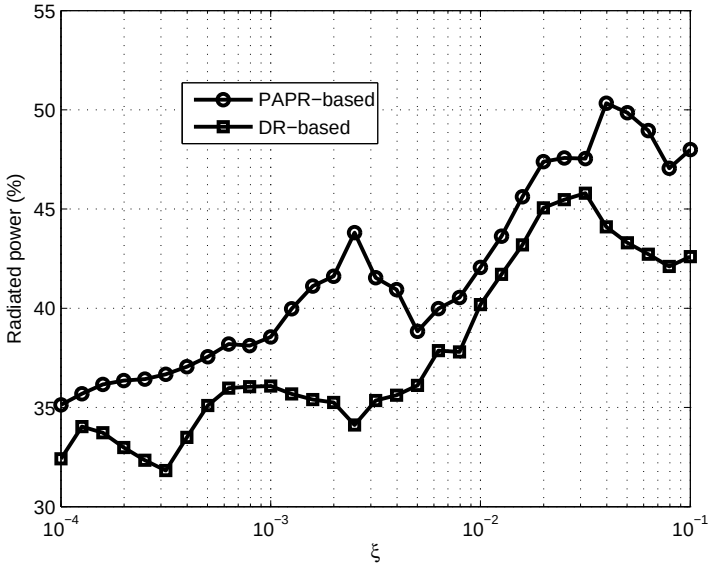

Fig. 4. Total radiated power v.s. ξ. $M = 16$.

It is interesting that for every 10 dB decrease in the ripple of generated broadbeam, the increment in dynamic range is by around 10 dB. This provides us a tradeoff between fluctuation in radiated pattern and dynamic range of antennas. Note that from (26) and (27), PAPR and DR depend on ξ nonlinearly. Therefore, we can find from Fig. 4 and Fig. 5 that the performance is not monotonous with ξ. Moreover, it is interesting that there are some local maxima of radiated power with respect to ξ. For instance, there is a local maximum around $\xi = 0.04$ with more than half of the total power radiated for the PAPR-based method. So, we also plot the associated beam pattern for the PAPR-based method in Fig. 6. Compared with Fig. 3, we can find that the increase in radiation power is at the expense of larger spikes in beam pattern, which may introduce larger inter-cell interference in cellular systems.

Since 2^{M-1} is very large for a large number of antennas, we here only show the optimal results for the case $M = 16$ due to the limitation in computing resource. We will also give an example of the ULA with $M = 128$ antennas. As suggested in Remark 3, we set the threshold for PAPR to be 8 dB, and break the loop (Step 6 of the algorithm in Table I) when the attained PAPR is close to 8 dB. The obtained beamforming vector for $\xi = 0.01$ is shown in Table II while Fig. 7 depicts the associated beam pattern,

This article has been accepted for publication in a future issue of this journal, but has not been fully edited. Content may change prior to final publication. Citation information: DOI 10.1109/TSP.2016.2521609, IEEE Transactions on Signal Processing

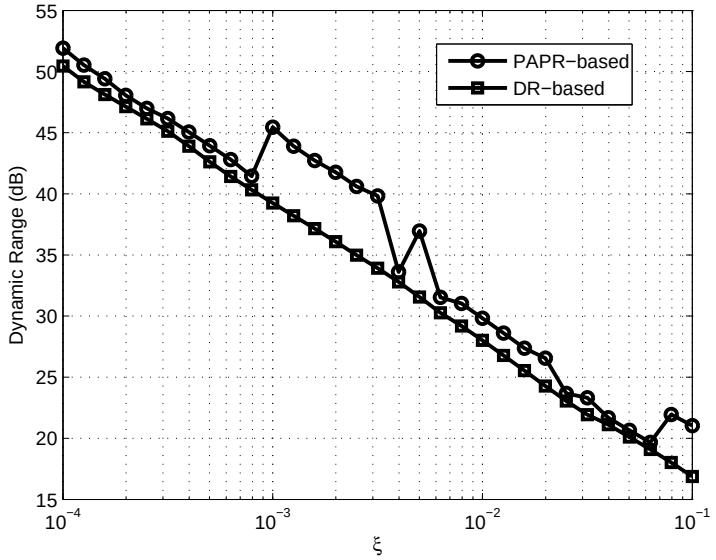

Fig. 5. Dynamic range v.s. ξ. $M = 16$.

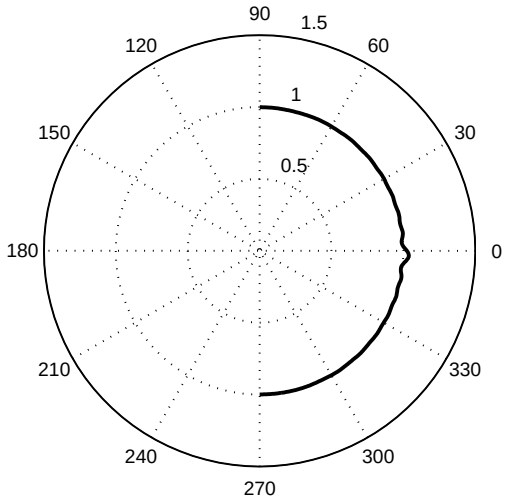

Fig. 6. Beam pattern. PAPR-based. $M = 16$.

This article has been accepted for publication in a future issue of this journal, but has not been fully edited. Content may change prior to final publication. Citation information: DOI 10.1109/TSP.2016.2521609, IEEE Transactions on Signal Processing

TABLE II
BEAMFORMING VECTOR. $M = 128$. $\xi = 0.01$.

m	v_m	m	v_m	m	v_m	m	v_m
1	0.0001	33	-0.0017 + 0.0005i	65	-0.0009 + 0.0019i	97	0.0018 - 0.0005i
2	0.0003 - 0.0002i	34	-0.0065 + 0.0088i	66	0.0022 + 0.0123i	98	0.0072 - 0.0089i
3	0.0004 - 0.0013i	35	0.0001 + 0.0359i	67	0.0301 + 0.0280i	99	0.0015 - 0.0376i
4	-0.0009 - 0.0025i	36	0.0435 + 0.0567i	68	0.0814 + 0.0080i	100	-0.0430 - 0.0612i
5	-0.0019 - 0.0012i	37	0.0583 + 0.0150i	69	0.0581 - 0.0370i	101	-0.0603 - 0.0183i
6	0.0029 - 0.0003i	38	-0.0700 + 0.0299i	70	-0.0297 + 0.0819i	102	0.0746 - 0.0282i
7	-0.0009 + 0.0009i	39	0.0157 - 0.0286i	71	-0.0115 - 0.0355i	103	-0.0177 + 0.0292i
8	- 0.0002i	40	0.0013 + 0.0062i	72	0.0061 + 0.0038i	104	-0.0010 - 0.0065i
9	0.0001 - 0.0003i	41	-0.0009 + 0.0018i	73	-0.0002 - 0.0012i	105	0.0003 + 0.0011i
10	-0.0003 - 0.0018i	42	0.0017 + 0.0118i	74	-0.0052 - 0.0051i	106	0.0053 + 0.0045i
11	-0.0042 - 0.0041i	43	0.0279 + 0.0278i	75	-0.0238 - 0.0033i	107	0.0228 + 0.0014i
12	-0.0116 - 0.0014i	44	0.0777 + 0.0101i	76	-0.0416 + 0.0235i	108	0.0378 - 0.0254i
13	-0.0085 + 0.0051i	45	0.0568 - 0.0336i	77	-0.0154 + 0.0372i	109	0.0119 - 0.0364i
14	0.0046 - 0.0116i	46	-0.0310 + 0.0775i	78	-0.0132 - 0.0491i	110	0.0162 + 0.0457i
15	0.0015 + 0.0051i	47	-0.0100 - 0.0343i	79	0.0174 + 0.0131i	111	-0.0175 - 0.0111i
16	-0.0009 - 0.0006i	48	0.0058 + 0.0038i	80	-0.0042 + 0.0003i	112	0.0040 - 0.0006i
17	-0.0003 - 0.0006i	49	0.0008 + 0.0010i	81	-0.0011 + 0.0007i	113	-0.0005 + 0.0001i
18	-0.0034 - 0.0021i	50	0.0073 + 0.0020i	82	-0.0028 + 0.0071i	114	-0.0022 + 0.0024i
19	-0.0132 + 0.0011i	51	0.0232 - 0.0092i	83	0.0066 + 0.0244i	115	-0.0011 + 0.0107i
20	-0.0195 + 0.0178i	52	0.0255 - 0.0426i	84	0.0399 + 0.0305i	116	0.0113 + 0.0183i
21	-0.0037 + 0.0219i	53	-0.0052 - 0.0415i	85	0.0423 - 0.0004i	117	0.0170 + 0.0062i
22	-0.0132 - 0.0248i	54	0.0372 + 0.0375i	86	-0.0421 + 0.0331i	118	-0.0218 + 0.0068i
23	0.0110 + 0.0049i	55	-0.0225 - 0.0029i	87	0.0055 - 0.0222i	119	0.0056 - 0.0081i
24	-0.0022 + 0.0007i	56	0.0037 - 0.0024i	88	0.0020 + 0.0040i	120	0.0002 + 0.0019i
25	-0.0011 - 0.0005i	57	-0.0011 - 0.0008i	89	-0.0007 - 0.0020i	121	- 0.0001i
26	-0.0073 + 0.0012i	58	-0.0084 - 0.0001i	90	-0.0104 - 0.0073i	122	-0.0005 - 0.0007i
27	-0.0169 + 0.0175i	59	-0.0223 + 0.0163i	91	-0.0417 + 0.0012i	123	-0.0026 - 0.0010i
28	-0.0056 + 0.0482i	60	-0.0155 + 0.0526i	92	-0.0644 + 0.0523i	124	-0.0053 + 0.0016i
29	0.0213 + 0.0348i	61	0.0170 + 0.0430i	93	-0.0156 + 0.0681i	125	-0.0027 + 0.0038i
30	-0.0482 - 0.0185i	62	-0.0502 - 0.0300i	94	-0.0369 - 0.0803i	126	-0.0003 - 0.0059i
31	0.0212 - 0.0065i	63	0.0248 - 0.0031i	95	0.0336 + 0.0174i	127	0.0016 + 0.0019i
32	-0.0023 + 0.0036i	64	-0.0033 + 0.0036i	96	-0.0071 + 0.0017i	128	-0.0005 - 0.0001i

where the PAPR of the beamforming vector is 8.1 dB.[2]

[2]Note that this is not the smallest PAPR for $M = 128$. For a faster computer with longer running time, we can have a smaller PAPR value.

This article has been accepted for publication in a future issue of this journal, but has not been fully edited. Content may change prior to final publication. Citation information: DOI 10.1109/TSP.2016.2521609, IEEE Transactions on Signal Processing

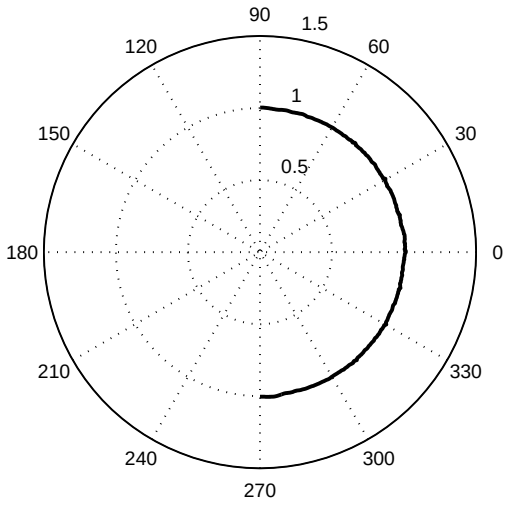

Fig. 7. Beam pattern. $M = 128$.

So far, we have provided results for the ULA. In Fig. 8(a), we plot the beam pattern for a 16×8 uniform rectangular array with $\Delta_a = \Delta_e = \frac{\lambda}{2}$, with Fig. 8(b) and 8(c) representing azimuth and elevation patterns for illustration. From the figures, the proposed method can apply to the uniform rectangular array as well.

B. CDF of SINR

Similar to [2], we consider a typical cellular network with 19 cells. We assume the ULA with half wavelength spacing for each base station located at the center of each cell. Assume that the cell radius is 1.6 km, the antenna number is $M = 128$, the number of users per cell is 10, and no user is located within 100 m of the base stations. The parameters for simulation are summarized in Table III. Here, we consider a Kronecker channel model as in [22]. The channel formed between user k in cell l and the BS in cell l' is given by

$$\mathbf{h}_{kll'} = \sqrt{\beta_{kll'}}\mathbf{R}^{\frac{1}{2}}\mathbf{g}_{iid}, \tag{40}$$

This article has been accepted for publication in a future issue of this journal, but has not been fully edited. Content may change prior to final publication. Citation information: DOI 10.1109/TSP.2016.2521609, IEEE Transactions on Signal Processing

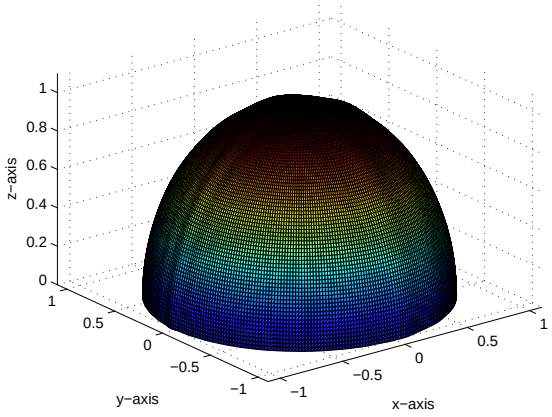

(a) Beam pattern.

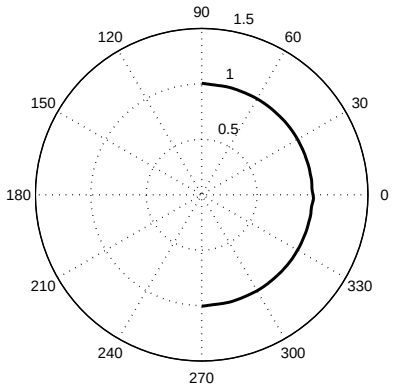

(b) Azimuth pattern.

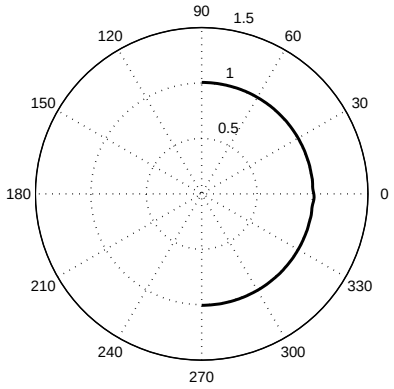

(c) Elevation pattern.

Fig. 8. Beam pattern for 16×8 URA.

This article has been accepted for publication in a future issue of this journal, but has not been fully edited. Content may change prior to final publication. Citation information: DOI 10.1109/TSP.2016.2521609, IEEE Transactions on Signal Processing

TABLE III
SIMULATION PARAMETERS.

BS power (P)	46 dbm
System Bandwidth (B)	20 MHz
Noise power density (N_0)	-174 dbm/Hz
Cell Radius	1600 m
Cell Hole	100 m
BS Antenna number	128
Antenna Configuration	ULA
Antenna Separation	$\frac{\lambda}{2}$
Number of UEs per Cell	10
UE Antenna number	1

where $\beta_{kll'}$ denotes the path loss with

$$\beta_{kll'} = \frac{1}{d_{kll'}^{\gamma}}, \tag{41}$$

where $d_{kll'}$ is the distance between base station l' and user k in cell l, and $\gamma \in (2, 4)$ is the path loss exponent, $\mathbf{R}$ represents the correlation matrix at the BS, and $\mathbf{g}_{iid} \sim \mathcal{CN}(\mathbf{0}, \mathbf{I})$, whose entries are independently identically distributed circularly symmetric complex Gaussian $\mathcal{CN}(0, 1)$. For the ULA antenna structure, $\mathbf{R}$ is Toeplitz, i.e., $\mathbf{R} = \mathbf{T}(\mathbf{J})$ with [22]

$$\mathbf{J} = \left[J_0(0), J_0\left(\frac{2\pi}{\lambda}\Delta\right), \ldots, J_0\left(\frac{2\pi}{\lambda}(M-1)\Delta\right) \right], \tag{42}$$

where $J_0(x)$ is the Bessel function of order 0. Note that the log-normal fading is not considered here.

We are interested in the received signal-to-interference-and-noise ratio (SINR). For the baseline, we consider the SINR obtained as if the base station is only equipped with one antenna sending signals with full power, termed as "Geometry". In this case, the received SINR of user k in cell l is defined as

$$\text{SINR}_{kl,geo} = \frac{\text{SNR}|h_{kll}|^2}{1 + \text{SNR}\sum_{l' \neq l} |h_{kll'}|^2}, \tag{43}$$

where $\text{SNR} = \frac{P}{N_0 B}$ denotes the transmit signal-to-noise ratio (SNR). If the antenna sends signal with maximum power of $\frac{1}{M}$, termed as "Single-Antenna", we have the received SINR for this case as

$$\text{SINR}_{kl,sing} = \frac{\text{SNR}|h_{kll}|^2}{M + \text{SNR}\sum_{l' \neq l} |h_{kll'}|^2}. \tag{44}$$

This article has been accepted for publication in a future issue of this journal, but has not been fully edited. Content may change prior to final publication. Citation information: DOI 10.1109/TSP.2016.2521609, IEEE Transactions on Signal Processing

If we assume that the base stations send signals with broadbeam in each cell, the received signal of user k in cell l for each symbol can be expressed as

$$y_{kl} = \underbrace{\mathbf{h}_{kll}^H \mathbf{v} s_l}_{\text{useful signal}} + \underbrace{\sum_{l' \neq l} \mathbf{h}_{kll'}^H \mathbf{v} s_{l'}}_{\text{inter-cell interference}} + n_{kl}, \tag{45}$$

where $\mathbf{v}$ denotes the beamforming vector generating the broadbeam, $s_l \sim \mathcal{CN}(0, P/B)$ denotes the signal sent by the base station in cell l, $n_{kl} \sim \mathcal{CN}(0, N_0)$ is the circularly symmetric complex Gaussian noise at the user side. Now, we can obtain the received SINR of user k in cell l as

$$\text{SINR}_{kl} = \frac{\text{SNR}|\mathbf{h}_{kll}^H \mathbf{v}|^2}{1 + \text{SNR} \sum_{l' \neq l} |\mathbf{h}_{kll'}^H \mathbf{v}|^2}. \tag{46}$$

Also, we consider random beamforming for sending control signaling, where the beamforming vector for base station l is generated by $\mathbf{v}_l \sim \mathcal{CN}(\mathbf{0}, \mathbf{I})$, whose entries are independently identically distributed circularly symmetric complex Gaussian $\mathcal{CN}(0, 1)$. We also assume peak power constraint such that $\mathbf{v}_l$ is further normalized by (29). Now, we can express the received SINR of user k in cell l as

$$\text{SINR}_{kl,rb} = \frac{\text{SNR}|\mathbf{h}_{kll}^H \mathbf{v}_l|^2}{1 + \text{SNR} \sum_{l' \neq l} |\mathbf{h}_{kll'}^H \mathbf{v}_{l'}|^2}. \tag{47}$$

In our simulation, we assume that the user terminals are uniformly distributed over the coverage area. We consider 10 drops, each with 10^3 instances of the channel coefficients. In Fig. 9, we plot the cumulative distribution function (CDF) of SINR with parameters defined in Table III. We assume that the beamforming vector shown in Table II is used for each base station in case of "Broadbeam". From the figure, we can find that the proposed broadbeam generation method performs close to the random beamforming and the one as if only one antenna sending with full power, and is much better than the one achieved with only antenna sending with power of $1/M$. The problem associated with random beamforming is that the generated beam pattern is not applicable in practical systems for coverage. We plot the beam pattern of a random beamforming vector in Fig. 10 as an example, where the radiated power fluctuated dramatically and becomes zero in certain directions. Then, it is possible that some users cannot receive the control signaling, e.g., line-of-sight (LOS) users in the directions without any radiation power.

This article has been accepted for publication in a future issue of this journal, but has not been fully edited. Content may change prior to final publication. Citation information: DOI 10.1109/TSP.2016.2521609, IEEE Transactions on Signal Processing

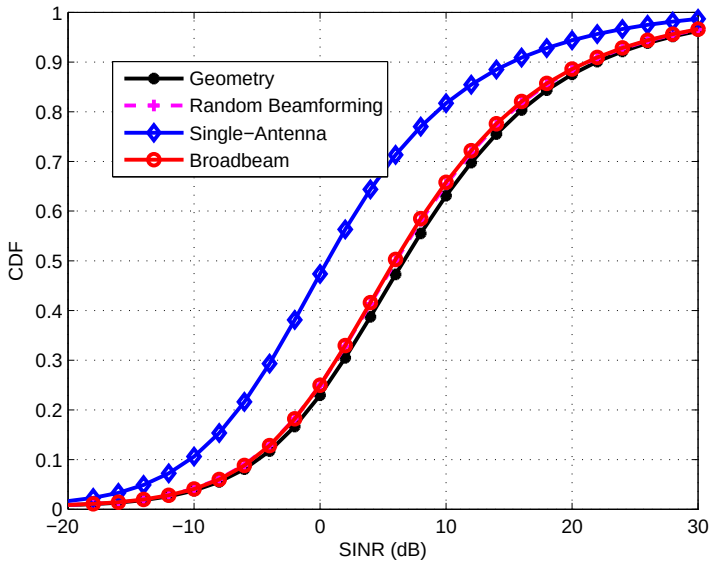

Fig. 9. CDF of the received SINR.

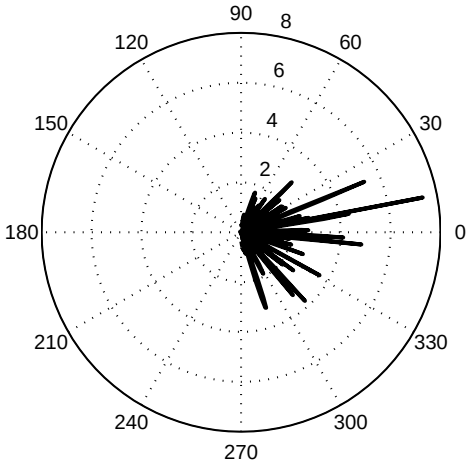

Fig. 10. Beam pattern for random beamforming. $M = 128$.

IV. Conclusions

In this paper, we have considered broadbeam generation in massive MIMO systems. We have shown that the only possible solutions to perfect broadbeam with identical radiated power in all directions are the unit vectors with only one nonzero element. Therefore, some fluctuation in transmit powers of different directions must be allowed. We have proposed a method to generate broadbeam that is almost flat in all directions while minimizing the PAPR or dynamic range for practical applications. We have also provided numerical results verifying our algorithm. Overall, we have offered a feasible solution to generating broadbeam of practical use in massive MIMO systems.

References

[1] Huawei Technologies, "5G: A Technology Vision, "*White Paper*, 2013. Available: www.huawei.com/ilink/en/download /HW_314849.

[2] T. Marzetta, "Noncooperative cellular wireless with unlimited numbers of base station antennas, "*IEEE Trans. on Wireless Commun.*, vol. 9, no. 11, pp. 3590 - 3600, Nov. 2010.

[3] L. Lu, G. Y. Li, A. L. Swindlehurst, A. Ashikhmin, and R. Zhang, "An overview of massive MIMO: Benefits and challenges," *IEEE J. Sel. Topics Sig. Proc.*, vol. 8, no. 5, pp. 742 - 758, May 2014.

[4] F. Boccardi, R.W. Heath, Jr., A. Lozano, T. Marzetta, and P. Popovski, "Five disruptive technology directions for 5G," *IEEE Commun. Mag.*, vol. 52, no. 2, pp. 74 - 80, Feb. 2014.

[5] E.G.Larson, O. Edfors, F. Tuvesson, and T. Marzetta, "Massive MIMO for next generation wireless systems, "*IEEE Comm. Mag.*, vol. 52, no. 2, pp. 186-195, Feb. 2014.

[6] F. Rusek, D. Persson, B. K. Lau, E. G. Larsson, T. L. Marzetta, O. Edfors, and F. Tufvesson, "Scaling up MIMO: Opportunities and challenges with very large arrays", *IEEE Signal Proces. Mag.*, vol. 30, no. 1, pp. 40-46, Jan. 2013.

[7] H. Huh, G. Caire, H.C. Papadopoulos, and S.A. Ramprashad, "Achieving "Massive MIMO" spectral efficiency with a not-so-large number of antennas, "*IEEE Trans. Wireless Comm.*, vol. 11, no. 9, pp. 3226 - 3239, Sep. 2012.

[8] S. K. Mohammed and E. G. Larsson, "Constant-envelope multi-user precoding for frequency-selective massive MIMO systems", *IEEE Wireless Commun. Lett.*, vol. 2, no. 5, pp. 547-550, Oct. 2013.

[9] C. Studer and E. G. Larsson, "PAR-aware large-scale multi-user MIMO-OFDM downlink", *IEEE J. Sel. Areas Commun.*, vol. 31, no. 2, pp. 303-313, Feb. 2013.

[10] H. Prabhu, O. Edfors, J. Rodrigues, L. Liu, F. Rusek, "A low-complex peak-to-average power reduction scheme for OFDM based massive MIMO systems", *IEEE Int. Symp. on Commun., Control and Signal Processing*, Athens, Greece, May 2014.

[11] E. Björnson, E. G. Larsson, T. L. Marzetta, "Massive MIMO: 10 myths and one grand question," submitted for publication. Available: http://arxiv.org/pdf/1503.06854v1.pdf.

[12] 3GPP Technical Specification TS 36.211, Evolved universal terrestrial radio access (E-UTRA); Physical channels and modulation, 2010.

[13] G. Xu *et. al*, "Full-dimension MIMO: Status and challenges in design and implementation, " in *2014 IEEE Commun. Theory Workshop (CTW)*, the Piscadera Bay, Curaçao, May 2014.

[14] D.R. Fuhrmann and G. San Antonio, "Transmit beamforming for MIMO radar systems using signal cross-correlation," *IEEE Trans. Aerospace and Elec. Systems*, vol. 44, no. 1, pp. 171-186, Jan. 2008.

[15] Y.-C. Wang, X. Wang, H. Liu, and Z.-Q. Luo, "On the design of constant modulus probing signals for MIMO radar," *IEEE Trans. Sig. Proc.*, vol. 60, no. 8, pp. 4432 - 4437, Aug. 2012.

[16] P. Stoica, J. Li, and Y. Xie, "On probing signal design for MIMO radar," *IEEE Trans. Sig. Proc.*, vol. 55, no. 8, pp. 4151-4161, Aug. 2007.

[17] H. He, P. Stoica, and J. Li, "Wideband MIMO systems: signal design for transmit beampattern synthesis," *IEEE Trans. Sig. Proc.*, vol. 59, no. 2, pp. 618-628, Feb. 2011.

[18] A. Hassanien and S.A. Vorobyov, "Transmit energy focusing for DOA estimation in MIMO radar with colocated antennas," *IEEE Trans. Sig. Proc.*, vol. 59, no. 6, pp. 2669-2683, June 2011.

[19] B. Friedlander, "On transmit beamforming for MIMO radar, "*IEEE Trans. Aerospace and Elec. Systems*, vol. 48, no. 4, pp. 3376-3388, Apr. 2012.

[20] A. Khabbazibasmenj, S. A. Vorobyov, and A. Hassanien, "Transmit radiation pattern invariance in MIMO radar with application to DOA estimation," *IEEE Sig. Proc. Letters*, vol. 22, no. 10, pp. 1609 - 1613, Oct. 2015.

[21] A. Kammoun *et al.*, "Preliminary Results on 3D Channel Modeling: From Theory to Standardization" *IEEE J. Sel. Areas Commun.*, vol. 32, no. 6, pp. 1219 - 1229, June 2014.

[22] Q.-U.-A. Nadeem, A. Kammoun, M. Debbah, and M.-S. Alouini, "A generalized spatial correlation model for 3D MIMO channels based on Fourier coefficients of power spectrums," *IEEE Trans. Sig. Proc.*, vol. 63, no. 14, pp. 3671-3686, July 2015.

[23] C. A. Balanis, *Antenna Theory: Analysis and Design*, 3rd ed. New York: Wiley, 2005.

Deli Qiao received the B.E. degree in electrical engineering from Harbin Institute of Technology in 2007, and the Ph.D. degree in electrical engineering from the University of Nebraska-Lincoln in 2012. Currently, he is a faculty at the East China Normal University. From 2012 to 2014, he worked in Huawei Technologies Inc., LTD as a research engineer, focusing on 5G techniques especially massive MIMO. His research interests are in the general areas of wireless communications, information theory, and signal processing. In 2011, he received the Maude Hammond Fling Fellowship from the University of Nebraska-Lincoln.

Haifeng Qian received the B.S. and M.S. degrees in algebraic geometry from the Department of Mathematics at East China Normal University, Shanghai, China, in 2000 and 2003, respectively, and the PhD degree from the Department of Computer Science and Engineering at Shanghai Jiao Tong University, Shanghai, China, in 2006. He is a professor of the Department of Computer Science, East China Normal University. His main research interests include cryptography, network security and algebraic geometry. He is currently serving as a reviewer of multiple international journals and academic conferences.

This article has been accepted for publication in a future issue of this journal, but has not been fully edited. Content may change prior to final publication. Citation information: DOI 10.1109/TSP.2016.2521609, IEEE Transactions on Signal Processing

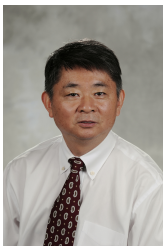

Geoffrey Ye Li (S'93-M'95-SM'97-F'06) received his B.S.E. and M.S.E. degrees in 1983 and 1986, respectively, from the Department of Wireless Engineering, Nanjing Institute of Technology, Nanjing, China, and his Ph.D. degree in 1994 from the Department of Electrical Engineering, Auburn University, Alabama.

He was a Teaching Assistant and then a Lecturer with Southeast University, Nanjing, China, from 1986 to 1991, a Research and Teaching Assistant with Auburn University, Alabama, from 1991 to 1994, and a Post-Doctoral Research Associate with the University of Maryland at College Park, Maryland, from 1994 to 1996. He was with AT&T Labs - Research at Red Bank, New Jersey, as a Senior and then a Principal Technical Staff Member from 1996 to 2000. Since 2000, he has been with the School of Electrical and Computer Engineering at the Georgia Institute of Technology as an Associate Professor and then a Full Professor. He is also holding a Cheung Kong Scholar title at the University of Electronic Science and Technology of China since 2006.

His general research interests include statistical signal processing and communications, with emphasis on cross-layer optimization for spectral- and energy-efficient networks, cognitive radios and opportunistic spectrum access, and practical issues in LTE systems. In these areas, he has published over 150 refereed journal and 200 conference papers in addition to 26 granted patents. His publications have been cited over 21,000 times and he has been recognized as the *World's Most Influential Scientific Mind*, also known as a *Highly-Cited Researcher*, by Thomson Reuters. He has been involved in editorial activities for over 20 technical journals for the IEEE Communications and Signal Processing Societies. He has organized and chaired many international conferences, including technical program vice-chair of *IEEE ICC'03*, technical program co-chair of *IEEE SPAWC'11*, general chair of *IEEE GlobalSIP'14* and technical program co-chair of *IEEE VTC'16 (Spring)*. He has been awarded IEEE Fellow for his contributions to *signal processing for wireless communications* since 2006. He won 2010 *Stephen O. Rice Prize Paper Award* and 2013 *WTC Wireless Recognition Award* from the *IEEE Communications Society* and 2013 *James Evans Avant Garde Award* and 2014 *Jack Neubauer Memorial Award* from the *IEEE Vehicular Technology Society*. Recently, he received *2015 Distinguished Faculty Achievement Award* from the *School of Electrical and Computer Engineering, Georgia Tech*.